

## Research Article

## POU4F3 Is a Sensitive and Specific Marker of Merkel Cell Carcinoma

 Pawel Karpinski<sup>a,\*</sup>, Javier E. Mendez-Pena<sup>b</sup>, Cheng-Lin Wu<sup>c</sup>, Ali Akalin<sup>d</sup>,  
 Kristine M. Cornejo<sup>b</sup>, Yin P. Hung<sup>b</sup>, Mai P. Hoang<sup>b,\*</sup>

<sup>a</sup> Department of Genetics, Wroclaw Medical University, Wroclaw, Poland; <sup>b</sup> Department of Pathology, Massachusetts General Hospital and Harvard Medical School, Boston, Massachusetts; <sup>c</sup> Department of Pathology, National Cheng Kung University Hospital, College of Medicine, National Cheng Kung University, Tainan, Taiwan; <sup>d</sup> Department of Pathology, UMass Medical Center, Worcester, Massachusetts

## ARTICLE INFO

## Article history:

Received 30 April 2024

Revised 4 September 2024

Accepted 20 September 2024

Available online 26 September 2024

## Keywords:

ASCL1

Merkel cell carcinoma

pou4f3

sentinel

lymph node

small cell lung carcinoma

## ABSTRACT

Although of therapeutic importance, a single sensitive and specific immunostain to distinguish Merkel cell carcinoma (MCC) from mimics is not currently available. In addition, single tumor cells are difficult to detect in sentinel lymph node biopsy. Leveraging publicly available data sets of 9264 solid tumors and >600,000 single-cell transcriptomes, we identified *POU4F3* to be a specific marker of MCC. Analyses of Pan-Cancer RNA bulk sequencing data of 24 tumor types from Tumor Cancer Genomic Atlas data sets as well as non-Tumor Cancer Genomic Atlas small cell lung carcinoma and MCC data sets confirmed *POU4F3* specificity for MCC. Single-cell RNA-sequencing analyses also confirmed the lack of *POU4F3* expression in lung small cell carcinoma as well as a variety of normal tissues. Nuclear *POU4F3* immunohistochemical expression was noted in 98.7% of 153 MCCs and in only 1.7% of mimics (3 of 180 cases, including 95 small cell carcinomas, of which 55 were from lungs and the remainder from other sites). Three *POU4F3*-positive non-MCC cases were from lungs (2 cases) and vagina (1 case). All 153 tested MCC cases were negative for ASCL1, a key transcriptional regulator highly expressed in small cell lung carcinoma. NeuroD1 was seen in a subset of MCC cases (20.9%, 32/153). *POU4F3* immunostain was performed on 29 sentinel lymph nodes, and strong *POU4F3* nuclear expression facilitated the ease of metastasis detection, even single tumor cells. Our study built on prior works shows that *POU4F3* is a sensitive and specific clinical marker of MCC.

© 2024 United States & Canadian Academy of Pathology. Published by Elsevier Inc. All rights are reserved, including those for text and data mining, AI training, and similar technologies.

## Introduction

Merkel cell carcinoma (MCC) is a rare yet deadly cutaneous tumor.<sup>1</sup> Although 40 times less common than melanoma, MCC is deadlier than melanoma with a historical mortality rate of approximately 33% to 46%.<sup>1</sup> Currently, it is accepted that there are 2 possible pathways for MCC pathogenesis. One is caused by the

clonal integration of the Merkel cell polyomavirus (MCPyV) into the neoplastic cells, and the other by ultraviolet irradiation.<sup>1</sup>

Distinguishing advanced MCC, especially the MCPyV-negative tumors from small cell lung carcinoma (SCLC) is of therapeutic importance. Although immunotherapy is the front-line treatment for advanced MCC, a combination of platinum and etoposide is the most widely used chemotherapy for SCLC.<sup>1,2</sup> The availability of MCPyV immunostain facilitates the identification of MCPyV-positive MCC. However, distinguishing MCPyV-negative MCC from high-grade neuroendocrine carcinomas (NECs) remains diagnostically challenging because they often share similar morphologic features and immunoprofiles. Both MCC and SCLC

\* Corresponding authors.

E-mail addresses: [pawel.karpinski@umw.edu.pl](mailto:pawel.karpinski@umw.edu.pl) (P. Karpinski), [mhoang@mg.harvard.edu](mailto:mhoang@mg.harvard.edu) (M.P. Hoang).



express keratins AE1/AE3, CAM5.2, and MNF116.<sup>3,4</sup> Although MCCs typically express paranuclear dot-like staining for keratin 20, this pattern can also be seen in NECs.<sup>5</sup> In addition, up to 24% of MCCs do not express keratin 20,<sup>6,7</sup> and TTF1 positivity can be seen, especially in MCPyV-negative MCCs.<sup>8</sup> An immunohistochemical panel including keratin 20, neurofilament, special AT-rich sequence-binding protein 2 (SATB2), MCPyV, and TTF1 together with clinical findings and imaging studies have been reported to be helpful in the distinction of MCC from high-grade NEC.<sup>9-11</sup> In a study of 103 MCC versus 70 extracutaneous NEC, Kervarrec et al reported neurofilament, SATB2, and MCPyV to be the most discriminant markers. Nevertheless, this panel of 3 immunostains would not detect MCPyV-negative MCC. Recently, Sox11 has been reported to be a helpful distinguishing marker because the majority of MCCs express strong and diffuse Sox11.<sup>12</sup> However, moderate and weak Sox11 expression can be seen in 38% and 24% of MCCs, respectively, and it has been identified in 7% of SCLCs.<sup>12</sup> As evident in the above reported findings, there is a need for additional sensitive and specific immunostains to distinguish MCCs from mimics in clinical laboratories.

In addition, with currently available immunostains, single and small clusters of tumor cells are difficult to detect in sentinel lymph node (SLN) biopsy. Due to focal keratin 20 staining, additional cytokeratins, usually consisting of either pankeratin or keratin AE1/AE3, are used to detect metastasis in SLN. However, background staining of fibroblasts and dendritic processes is frequently observed with cytokeratin.<sup>13</sup> A recent study suggested a combination of SATB2 and keratin AE1/AE3 to be helpful in the workup of metastatic MCC, although background staining is frequently seen with SATB2.<sup>14</sup>

In this study, we aimed to identify an immunohistochemical marker that is sensitive and specific for MCC. First, we explored possible distinguishing gene expression profiles of MCC and SCLC by analyzing publicly available RNA-sequencing data. We then validated gene expression results with protein expression and assessed the sensitivity and specificity of the potential immunohistochemical markers. We also evaluated the potential utility of the immunostain in detecting single-cell metastasis in SLN biopsy.

## Methods

### RNA-Sequencing Analyses

#### External Data Acquisition

**Bulk Tumor Data.** RNA-seq single-end MCC data consisting of 107 bulk tumor samples (35 MCPyV-negative and 72 MCPyV-positive) were downloaded as FASTQ files from the Sequence Read Archive (SRA) database in National Center for Biotechnology Information (NCBI) accessed under the BioProject PRJNA775071.<sup>15</sup> RNA-seq paired-end data for 16 SCLCs and 10 lung adenocarcinoma tumors (named in this work lung adenocarcinoma [LUAD], external LUAD data set [LAUDex]) were downloaded as FASTQ files from ArrayExpress portal (EMBL-EBI) database, accession number: E-MTAB-10399.<sup>16</sup> Preprocessed the Cancer Genome Atlas (TCGA) pancancer RNA-seq data (raw counts) of 9264 samples representing 24 tumor subtypes (adrenocortical carcinoma, bladder urothelial carcinoma, breast invasive carcinoma, cervical squamous cell carcinoma, colon adenocarcinoma [COAD], diffuse large B-cell lymphoma, glioblastoma multiforme, head and neck squamous cancer, kidney chromophobe, kidney renal clear cell carcinoma, kidney renal papillary cell carcinoma, acute myeloid leukemia,

brain lower grade glioma, liver hepatocellular carcinoma, LUAD, lung squamous cell carcinoma, ovarian serous cystadenocarcinoma, prostate adenocarcinoma, rectum adenocarcinoma [READ], skin cutaneous melanoma, stomach adenocarcinoma, thyroid carcinoma, uterine corpus endometrial carcinoma, and uterine carcinosarcoma) were downloaded from the Gene Expression Omnibus database, accession number: GSE62944.<sup>17</sup> Cancer type abbreviations are provided in [Supplementary Table S1](#).

**POU4F3** expression in 17,382 RNA-sequencing samples from 54 tissues of 948 postmortem donors was assessed and visualized in the Adult Genotype Tissue Expression Project portal (Release V8 [dbGaP Accession phs000424.v8.p2]).<sup>18</sup>

### Single-Cell RNA-Seq Data

Preprocessed single-cell RNA-seq profiling (raw counts) of 11 patient-derived MCC samples (64,527 cells in total), comprised of 5 lymph node metastases, 5 primary cutaneous tumors, and 1 parotid gland metastasis was downloaded from the Gene Expression Omnibus database, accession number: GSE226438.<sup>19</sup>

Single-cell RNA-seq profiling of patient-derived SCLC samples (77,143 cells in total) comprising 9 primary SCLC tumors, 6 lymph node metastases, 3 liver metastases, 1 adrenal gland metastasis, and 1 axillary soft tissue metastasis was downloaded from the Human Tumor Atlas Network (<https://datasets.cellxgene.cziscience.com/7a30310a-2239-4d84-b99e-a12456c2fe19.rds>).<sup>20</sup>

Tabula sapiens single-cell atlas of nearly 500,000 cells from 24 organs of 15 healthy individuals was downloaded as the Seurat object from the Tabula sapiens portal (<https://tabula-sapiens-portal.dsczbiohub.org>).<sup>21</sup>

### Data Preprocessing

FASTQ files were subjected to quality filtering using the Rfastp Bioconductor package (version 1.10.0; <https://doi.org/10.18129/B9.bioc.Rfastp>). Filtered reads were aligned with the Rsubread Bioconductor package (version 2.14.2) to the human reference genome (GENCODE Release 43 [GRCh38.p13]) to produce Binary Alignment Map (BAM) files. Subsequently aligned reads were summarized to read counts (raw counts) using Rsubread Bioconductor package and GENCODE Release 43 (GRCh38.p13) gene annotation.<sup>22,23</sup>

To merge bulk tumor data obtained from MCCs, SCLCs, LUAD, and Pan-cancer TCGA, the raw counts data were merged based on the gene names. Next, lowly expressed genes were discarded by using filterByExpr() function in the edgeR package (version 3.42.4).<sup>24</sup> Merged data were then transformed to Seurat object followed by SCTransform normalization ("glmGamPoi" method and "v2" VST flavor) in Seurat Bioconductor package (version 4.4.0).<sup>25</sup> External LAUDex was used to assess whether normalization has efficiently removed batch effects without removing biological variability, allowing for the aggregation of external LUAD and TCGA LUAD tumors.

Single-cell RNA-seq data were transformed to Seurat object followed by filtering for cells containing a minimum of 200 and no more than 8000 unique genes and containing <10% mitochondrial genome. Filtered data were normalized using global-scaling normalization method "LogNormalize" (scale.factor = 10,000) in Seurat Bioconductor package (version 5.0.0).<sup>25</sup> All single-cell sequencing data sets were integrated across

treatment naïve samples using canonical correlation analysis (CCAIntegration method).<sup>25</sup>

### Statistical Analyses

We used sct-transformed MCCs and SCLCs data followed by a 2-step procedure to find a set of best markers in the distinction of MCC versus SCLC. First, we applied the nearest template prediction classifier to find top 40 differentially expressed (DE) genes between MCCs and SCLCs (log-fold change  $\geq 2$  and false discovery rate  $\leq 0.05$  thresholds) by using subDEG() function in CMScaller R package (version 2.0.1).<sup>26</sup>

Subsequently, the top 40 DE genes were narrowed down to the most discriminative ones using the partial least squares discriminant analysis algorithm implemented in mixOmics R package (version 6.24.0).<sup>27</sup> In brief, sct-transformed data narrowed to 40 DE genes were used as an input. We used the repeated cross-validation approach (10-fold cross-validation repeated 100 times) to identify small subsets of genes relevant to tumor type discrimination. We selected DE genes that were most often (with frequency = 1) selected across the folds during the repeated cross-validation process.

To visualize single-cell RNA-seq data, we selected the top 2000 variable features identified using the variance stabilizing transformation (VST) method. The data were scaled next; then, principal component analysis was performed. Thereafter, the elbow plot method was used to select the number of principal components for Unifold Manifold Approximation and Projection nonlinear dimensionality reduction. The k-nearest neighbor graph and Louvain clustering were then calculated.<sup>25</sup> DimPlot(), FeaturePlot(), and DotPlot() functions were used for visualizing gene(s) expression in low-dimensional space.

In GSE226438 single-cell RNA-seq data set, the cell types were not annotated; therefore, we used csSorter R package (version 0.0.2), a list of well-established canonical markers (Supplementary Table S2), and a guide provided by Das et al.<sup>19</sup> to identify cell types (Merkel cells, B cells, T cells, cancer-associated fibroblast, and monocytes) in the MCC data set.<sup>28</sup> The “unknown” category represents cells that could not be assigned to one of the 5 cell populations.

### Immunohistochemistry

Tissue microarrays were constructed for 257 cases including 137 MCCs, 51 SCLCs, 36 basal cell carcinomas, 22 metastatic melanomas, and 11 malignant peripheral nerve sheath tumors. Whole slide tissue sections were obtained for 105 cases, of which 16 were MCC tumors (either keratin 20-negative or TTF1-positive), 29 SLNs of MCC patients, and 60 non-MCC tumors. Immunohistochemical studies were performed on 5- $\mu$ m-thick tissue sections using a Bond 3 automated immunostainer (Leica Microsystems), with primary antibodies against POU4F3 (QQ8, 1:200, Santa Cruz Biotechnology), ASCL1 (E5S4Q, 1:100, Cell Signaling, Cat# 10585), NeuroD1 (EPR17084, 1:50, Abcam, Cat# ab205300), MCPyV large T-antigen (CM2B4, 1:100, Santa Cruz Biotechnology, sc-136172), keratin 20 (ks20.8, prediluted, Leica Microsystems), keratin AE1/AE3 (ae1/ae3, 1:800, Leica Microsystems), synaptophysin (27g12, prediluted, Leica Microsystems), POU2F3 (E5N2D, 1:500, Cell Signaling), and YAP1 (D8H1X, 1:200, Cell Signaling). The staining was scored independently by 2 co-authors, and discrepancies were resolved via consensus. The

scoring was based on percent positivity: 3+, >80%; 2+, 40% to 80%; 1+, 5% to <40%; and 0, <5%.

### Determination of Sensitivity and Specificity of POU4F3 in Detecting Merkel Cell Carcinoma

POU4F3 immunostains were performed on tissue microarrays of 137 MCCs, 51 SCLCs, 36 basal cell carcinomas, 22 metastatic melanomas, and 11 malignant peripheral nerve sheath tumors and on 105 whole slide sections of 16 MCCs, 29 SLNs from 15 patients with MCCs, 44 small cell carcinomas (4 SCLCs, 12 cervix, 3 vagina, 3 endometrium, 6 salivary gland/head and neck, 11 bladder, 3 prostate, 1 pancreas, and 1 gallbladder), 3 trichoblastomas, 3 Ewing sarcomas, 1 alveolar rhabdomyosarcoma, 4 synovial sarcomas, 2 T-cell lymphoblastic lymphomas, and 3 NUT carcinomas (Table 1). These tumors were retrieved from the pathology archival files of Massachusetts General Hospital, Boston, MA; UMass Medical Center, Worcester, MA; and National Cheng Kung University Hospital, College of Medicine, Tainan, Taiwan.

### Distinction of Merkel Cell Carcinoma Versus Small Cell Carcinoma

POU4F3, ASCL1, and NeuroD1 were performed on 137 MCCs and 51 SCLCs (Table 2). POU2F3 and YAP1 were performed on 51 SCLCs.

## Results

### RNA-Sequencing Analyses

#### Selection of Discriminative Genes Between Merkel Cell Carcinomas and Small Cell Lung Carcinomas

To precisely identify highly discriminative genes between MCC and SCLC at the mRNA level, we used a 2-step procedure on PRJNA775071 (35 MCPyV-negative and 72 MCPyV-positive MCCs) and E-MTAB-10399 (16 SCLCs) data sets. In the first step, using the Nearest Template Prediction (NPT) classifier, top 40 DE protein-coding genes were selected (Fig. 1). In the second step, the group of 40 selected markers was narrowed down by cross-validation to 6 genes that were most often selected across the folds (with frequency = 1).<sup>15,16</sup> Six genes were specifically and highly expressed in MCCs (RPL27A, RPS14, GSTP1, POU4F3, RPLP1, and TAGLN2) (Supplementary Fig. S1).

Supplementary Figure S2 illustrates that through normalization, SCTransform efficiently removed batch effects without eliminating biological variability, as evidenced by the joint aggregation of external LUAD and TCGA LUAD tumors. After successful pan-cancer data integration, we assessed the specificity of expression of the 6 selected genes and 6 additional genes previously reported to display MCC-specific expression (ATOH1, SOX2, ISL1, KRT20, TFAP2B, and CEACAM6) in pan-cancer settings.<sup>17</sup> Using merged data of 9264 tumors of 24 cancer subtypes (Supplementary Table S1), MCCs, and SCLCs, we found that all 12 genes showed the highest expression in MCC tissues; however, POU4F3, ATOH1, and ISL1 showed relatively low level of background expression in significant fraction of tumor types (Supplementary Fig. S3, Fig. 2). Moreover, 3 of 12 genes have shown prominent expression levels in other tumor types: KRT20 in colorectal cancers (COAD and READ), RPLP1 in ovarian cancer, and diffuse large B-cell lymphoma, GSTP1 in head and neck squamous cancer, and cervical squamous cell carcinoma (Supplementary Fig. S3, Fig. 2). Further analyses of 3 best-performing genes (POU3F4, ATOH1, and ISL1) in

**Table 1**

Summary of POU4F3 expression in Merkel cell carcinomas and histologic mimics

Tumor type	N	POU4F3			
		Positive	3+	2+	Negative
Merkel cell carcinoma	153	151/153 (98.7%)	149	2	2
MCPyV-positive	82	82/82	81	1	0
MCPyV-negative	71	69/71	68	1	2
Keratin 20-negative	10	9/10	9	0	1
Keratin 20 focally positive	12	12/12	12	0	0
TTF1-positive	8	8/8	8	0	0
Non-Merkel cell carcinoma cases	180	3/180 (1.7%)			
Small cell carcinoma, total	95	3/95 (3.2%)	0	2	92
Small cell carcinoma of lung	55	2/55	0	2	53
Small cell carcinoma of cervix	12	0/12	0	0	12
Small cell carcinoma of vagina	3	1/3	1	0	2
Small cell carcinoma of endometrium	3	0/3	0	0	3
Small cell carcinoma of salivary gland/head and neck	6	0/6	0	0	6
Small cell carcinoma of bladder	11	0/5	0	0	11
Small cell carcinoma of prostate	3	0/1	0	0	3
Small cell carcinoma of pancreas	1	0/1	0	0	1
Small cell carcinoma of gallbladder	1	0/1	0	0	1
Ewing sarcoma	3	0/3	0	0	3
Rhabdomyosarcoma, alveolar	1	0/1	0	0	1
Synovial sarcoma, poorly differentiated	4	0/4	0	0	4
Lymphoblastic lymphoma	2	0/2	0	0	2
NUT carcinoma	3	0/3	0	0	3
Trichoblastoma	3	0/3	0 <sup>a</sup>	0	3
Basal cell carcinoma	36	0/36	0	0	36
Metastatic melanoma	22	0/22	0	0	22
Malignant peripheral nerve sheath tumor	11	0/11	0	0	11

MCPyV, Merkel cell polyomavirus.

<sup>a</sup> Positive intratumoral Merkel cells in all 3 cases.

tumors representing gastrointestinal tract and SCLCs revealed increased expression of *ATOH1* in some SCLCs, colorectal (COAD and READ) and gastric (stomach adenocarcinoma) tumors, and increased expression of *ISL1* in SCLCs when compared with *POU3F4* (Fig. 2, Supplementary Fig. S3C). We therefore removed 11 of 12 marker genes and only analyzed *POU4F3* in downstream analyses.

### Single-Cell RNA Sequencing

#### *POU4F3* Is Expressed in Primary Merkel Cell Carcinomas Tumors and Metastases

Next, we investigated the cellular specificity of *POU4F3* expression in primary and metastatic MCCs of 11 patients at single-cell resolution using GSE226438 data set (Fig. 3).<sup>19</sup> In total, 59,129 cells were analyzed. We found that *POU4F3* is specifically expressed in neoplastic Merkel cells regardless of the tissue source (skin, lymph node metastasis, and parotid gland metastasis). No expression of *POU4F3* could be detected in B cells, T cells, cancer-associated fibroblasts, and monocytes.

**Table 2**

Merkel cell carcinoma versus small cell lung carcinoma

Immunostains	All MCC	SCLC	P value (vs SCLC)
POU4F3	151/153 (98.7%)	2/51 (3.9%)	<.0001
ASCL1	0/153 (0%)	45/51 (88%)	<.0001
NeuroD1	32/153 (20.9%)	29/51 (56.9%)	<.0001

Fisher exact test, 2-tailed P value, statistically significant P value &lt;.05.

MCC, Merkel cell carcinoma; MCPyV, Merkel cell polyomavirus; SCLC, small cell lung carcinoma.

#### *POU4F3* Is not Expressed in Primary Small Cell Lung Carcinoma Tumors and Small Cell Lung Carcinoma Metastases and Healthy Human Tissues

Using single-cell RNA-seq data obtained from 77,143 cells of 9 primary SCLC tumors, 6 lymph node metastases, 3 liver metastases, 1 adrenal gland metastasis, and 1 axillary soft tissue metastasis, we did not detect *POU4F3* expression in SCLC (data not shown).<sup>20</sup> We also did not detect *POU4F3* expression in a single-cell atlas of 483,000 cells from 24 organs of 15 healthy individuals (Supplementary Fig. S4).<sup>21</sup> In addition, *POU4F3* displayed very low expression levels in 17,382 RNA-sequencing samples from 54 tissues of 948 postmortem donors. The median expression levels for each tissue did not exceed 0.25 transcripts per kilobase million (Supplementary Fig. S5).<sup>18</sup>

### Validation of RNA-Seq Results by Immunohistochemistry

#### Transcription Factor *POU4F3* Distinguishes Merkel Cell Carcinomas From Histologic Mimics

One hundred fifty-three primary MCCs were from 153 patients whose ages ranged from 49 to 95 years (median: 76 years). There were 94 men and 59 women. Eighty-two of 153 (53.6%) MCCs were MCPyV-positive, and 71 of 153 (46.4%) were MCPyV-negative. Of cases with immunohistochemistry performed during clinical workup, keratin 20 expression was seen in 116 of 126 (92%), keratin AE1/AE3 in 39 of 40 (97.5%), pankeratin in 31 of 31 (100%), keratin 903 in 5 of 5 (100%), keratin CAM5.2 in 24 of 26 (92%), synaptophysin in 92 of 93 (99%), chromogranin in 72 of 84 (86%), and TTF1 in 8 of 72 (11%). DNA of 7 MCPyV-negative MCCs included in this study have been previously sequenced, and they demonstrated an ultraviolet light signature (*TP53* and *RB1*



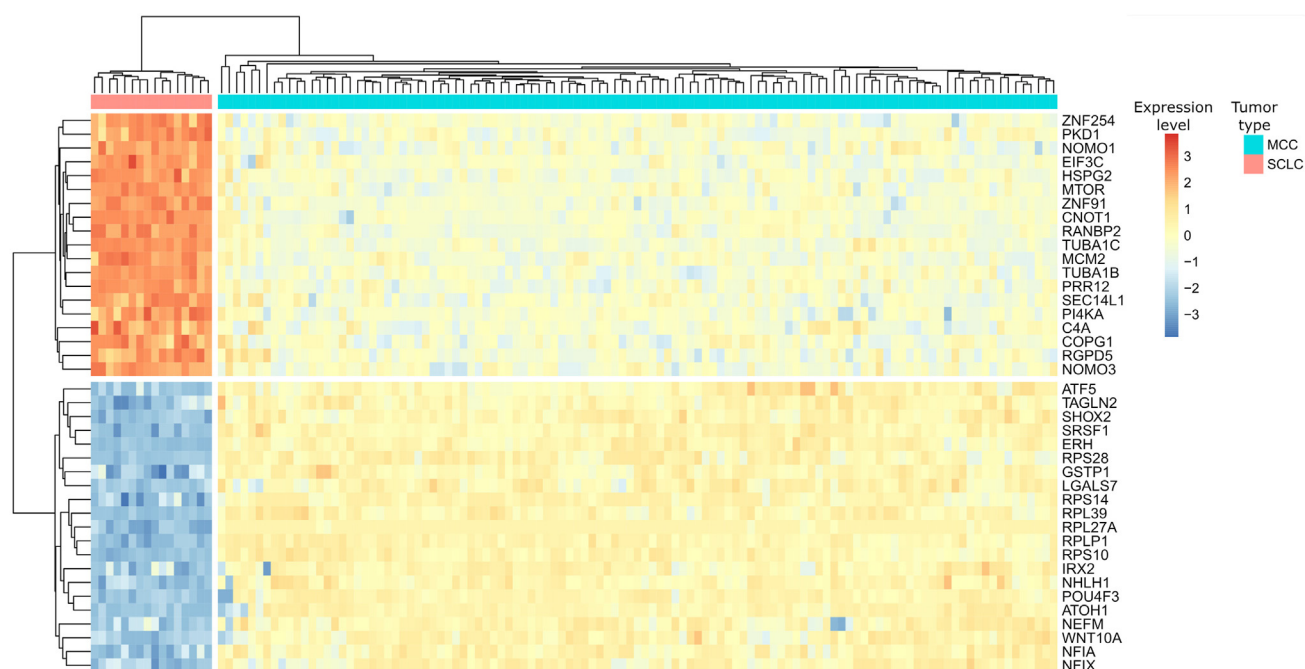


**Figure 1.**

Heatmap of top 40 differentially expressed genes in a comparison of Merkel cell carcinoma versus small cell lung carcinoma samples. MCC, Merkel cell carcinoma; SCLC, small cell lung carcinoma.

mutations) characteristic of MCC.<sup>29</sup> All 7 cases exhibited POU4F3 nuclear positivity, 3+ in 80% to 100% of the tumor cells.

The immunohistochemical expression of POU4F3 in 153 MCCs and 180 non-MCC tumors is summarized in Table 1. Of the 151 POU4F3-positive MCC cases, 3+ staining was seen in 97.4% (149/153) of cases, and 2+ staining was seen in 1.3% (2/153) of cases (Fig. 4). Eighty-two of 82 (100%) MCPyV-positive MCCs and 69/71 (97%) MCPyV-negative MCCs expressed POU4F3 (Table 1). Nine of 10 keratin 20-negative, 12 of 12 focally keratin 20-positive, and 8 of 8 TTF1-positive MCCs expressed POU4F3 (Table 1). The 1 keratin-20 negative MCC that did not express POU4F3 has a pleomorphic morphology with multinucleated and giant tumor cells.

POU4F3 expression was seen in only 3 of 180 (1.7%) non-MCC cases. POU4F3 was seen in 2 pulmonary SCLC with 2+ positivity (1 coexpressed ASCL1 and TTF1 and the other NeuroD1 and TTF1) and 1 vaginal small cell carcinoma with 3+ positivity (negative for both ASCL1 and NeuroD1). POU4F3 was not expressed in remaining small cell carcinomas, other small round blue cell tumors (Ewing sarcoma, alveolar rhabdomyosarcoma, poorly differentiated synovial sarcoma, T-cell lymphoblastic lymphoma, and NUT carcinoma), basal cell carcinoma, metastatic melanoma, and malignant peripheral nerve sheath tumor (Table 1, Supplementary Fig. S6). Background staining was not seen. Stromal cells, endothelial cells, and inflammatory cells were all negative. In 3 trichoblastomas, a cutaneous follicular tumor known to have intratumoral keratin 20-positive Merkel cells, POU4F3 highlights many intratumoral Merkel cells (Supplementary Fig. S7). By immunohistochemistry, we confirmed that POU4F3 is a sensitive and specific marker of MCC, with a sensitivity of 98.7% and a specificity of 98.3%.

#### *POU4F3 Is a Sensitive Marker for Merkel cell carcinomas and Helpful in the Distinction From Small Cell Lung Carcinoma*

A panel of POU4F3, ASCL1, and NeuroD1 was performed on 153 MCCs and 51 SCLCs. POU2F3 and YAP1 were performed on 51 SCLCs. ASCL1, NeuroD1, POU2F3, and YAP1 were positive in 45, 29, 2, and 3 cases, respectively. ASCL1-dominant staining was noted in

38 of 51 (74.5%) SCLCs. NeuroD1-dominant staining was noted in 12 of 51 (23.5%) SCLCs. POU2F3 expression with double ASCL1 and NeuroD1 negativity was noted in 1 of 51 (2%) SCLCs. Statistical significance was observed for all comparisons of MCC versus SCLC (Table 2). In the detection of SCLC, the sensitivity of ASCL1 is 88%, and its specificity is 100%. Although 45 of 51 (88%) of SCLCs were positive for ASCL1, none of the 153 MCCs expressed ASCL1 (Fig. 4). There is an overlapping staining pattern for NeuroD1 in MCC and SCLC with expression seen in 20.9% (32/153) and 56.9% (29/51), respectively (Fig. 4, Table 2).

#### *POU4F3 Is a Helpful Marker in Sentinel Lymph Node Evaluation*

Twenty-nine SLN biopsies were from 15 patients whose ages range from 64 to 85 years (median: 78 years) with a male:female ratio of 4:1. The primary tumor sites were head and neck (7), trunk (4), and extremities (4) (Supplementary Table S3). A clinical protocol comprised of keratin 20, keratin AE1/AE3, and synaptophysin was previously done in all studied 29 SLNs. In 12 of 21 positive lymph nodes, the size of the metastases ranged from 0.5 to 7 mm (median: 4 mm). The metastases were comprised of single tumor cells in the remaining 8 positive cases. Nine SLNs were negative.

POU4F3 was performed on all 29 SLNs and was strongly expressed in all 20 cases positive with keratin 20, keratin AE1/AE3, and synaptophysin. In 12 cases with macrometastases, strong nuclear expression of POU4F3 was seen in all cases (Fig. 5, case 1). Although positive, dot-like positivity was noted for keratin 20 and keratin AE1/AE3 is weaker in intensity in comparison with nuclear POU4F3 expression (Fig. 5, case 2). In addition, background staining is not seen in POU4F3, which is often noted for keratin AE1/AE3. In 9 cases with single-cell metastases, weak synaptophysin expression and dot-like positivity for keratin 20 and keratin AE1/AE3 are often noted, requiring careful examination of the SLN at high magnification. For these reasons, strong nuclear POU4F3 expression facilitates ease in the detection of metastasis, even single metastatic tumor cells (Fig. 5, cases 2 and 3). In one of 9 cases previously classified as negative by SLN protocol, POU4F3

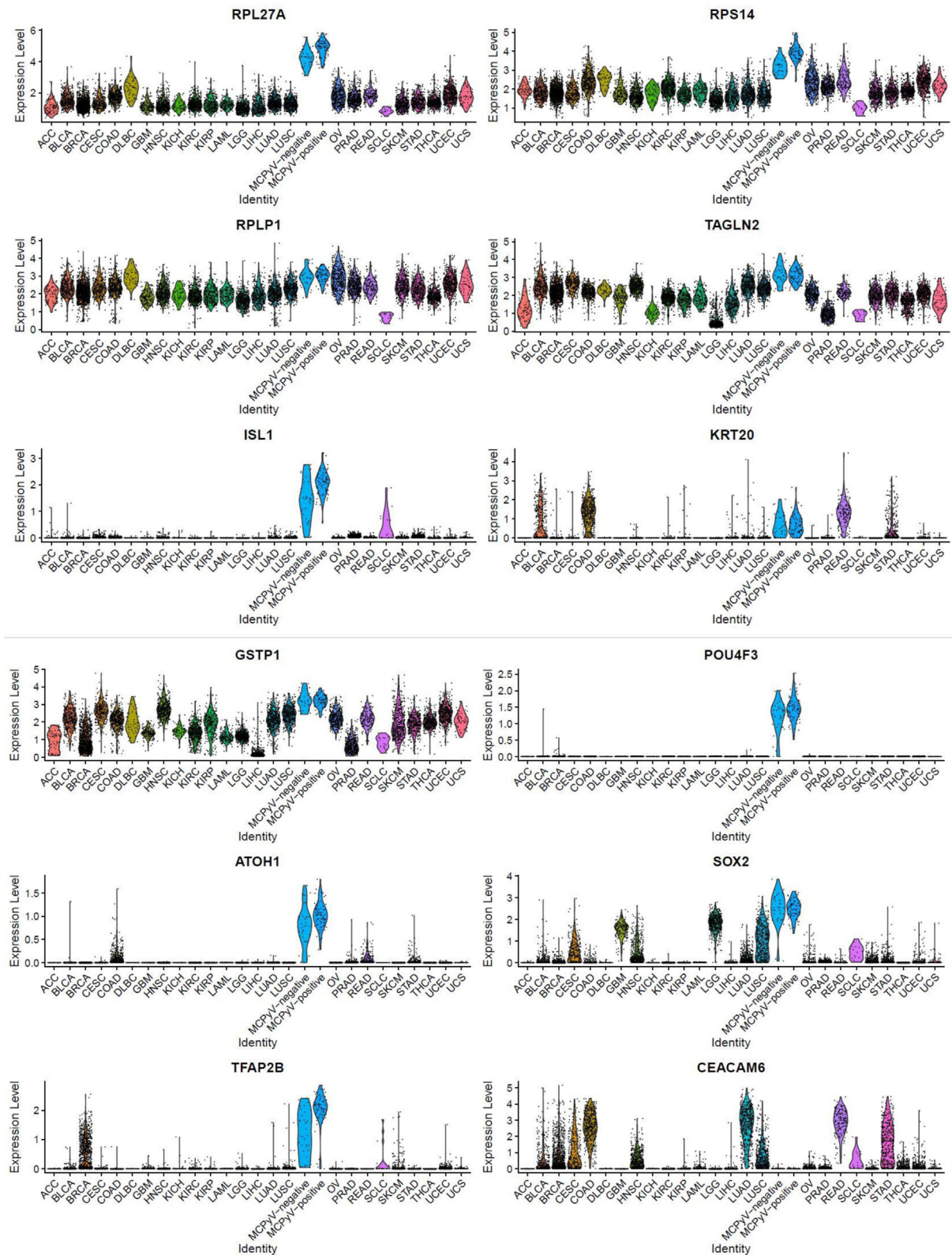


**Figure 2.**

Pancancer expression of selected genes expressed specifically in MCCs when compared with SCLCs (GSE62944, PRJNA775071, and E-MTAB-10399). Violin plot visualization of 6 selected genes (*RPL27A*, *RPS14*, *GSTP1*, *POU4F3*, *RPLP1*, and *TAGLN2*) and 6 additional genes previously reported to display MCC-specific expression (*ATOH1*, *SOX2*, *ISL1*, *KRT20*, *TFAP2B*, and *CEACAM6*) in pancancer setting. Abbreviations can be found spelled out in [Supplementary Table S1](#). Note, low frequency of expression of *POU4F3* in other tumors than MCC when compared with the other genes. Note increased expression of *ATOH1* in colon, rectal and gastric tumors and increased expression of *ISL1* in SCLCs when compared with *POU4F3*. MCC, Merkel cell carcinoma; SCLC, small cell lung carcinoma.



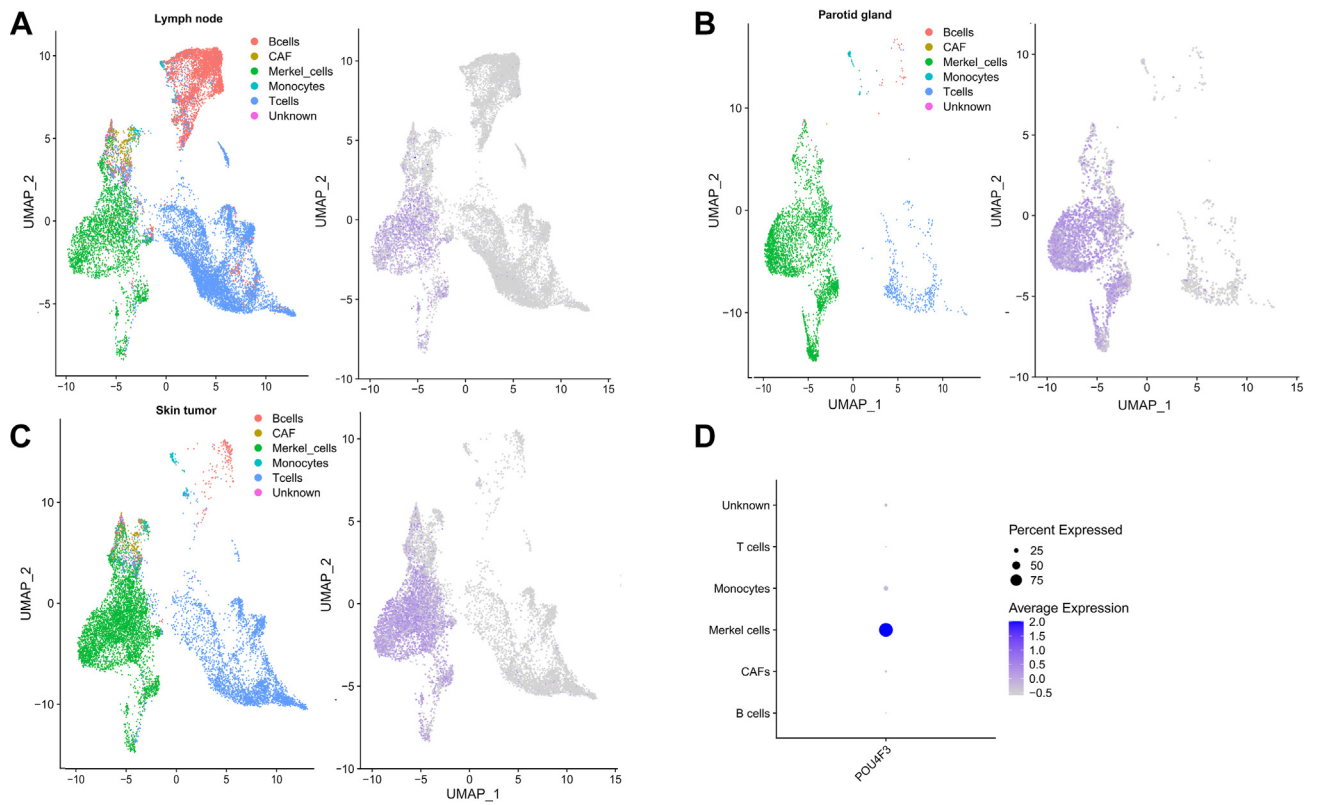


**Figure 3.**

Unifold Manifold Approximation and Projection visualization of *POU4F3* expression in treatment naïve MCC tumor tissues split to 5 cell populations (tumor Merkel cells, B cells, T cells, cancer-associated fibroblasts and monocytes) (GSE226438). The data were integrated across samples. (A) 5 lymph node metastases, (B) 1 parotid gland metastasis, (C) 5 primary skin tumors, and (D) dot plot summarizing *POU4F3* expression in 5 cell populations and 3 tissues. "Unknown" category represents cells that could not be assigned to one of 5 cell populations. Dot radius represents percent of tumors expressing given gene. Color intensity of dots reflects level of expression of given gene. MCC, Merkel cell carcinoma.

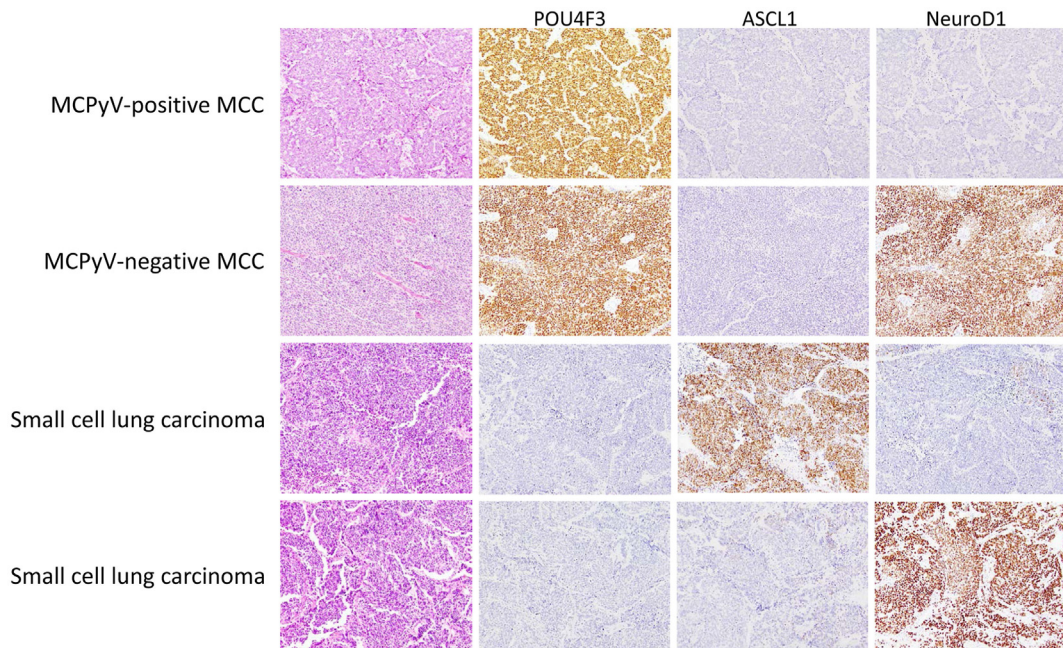


**Figure 4.**

Expression of *POU4F3*, *ASCL1*, and *NeuroD1* in MCPyV-positive and MCPyV-negative Merkel cell carcinoma, and small cell lung carcinoma. *POU4F3* is strongly positive in both MCPyV-positive and MCPyV-negative Merkel cell carcinomas, whereas it is negative in small cell lung carcinoma. *ASCL1* expression is seen mainly in small cell lung carcinoma. *NeuroD1* expression can be seen in subsets of both small cell lung carcinoma and Merkel cell carcinoma. MCC, Merkel cell carcinoma; MCPyV, Merkel cell polyomavirus.

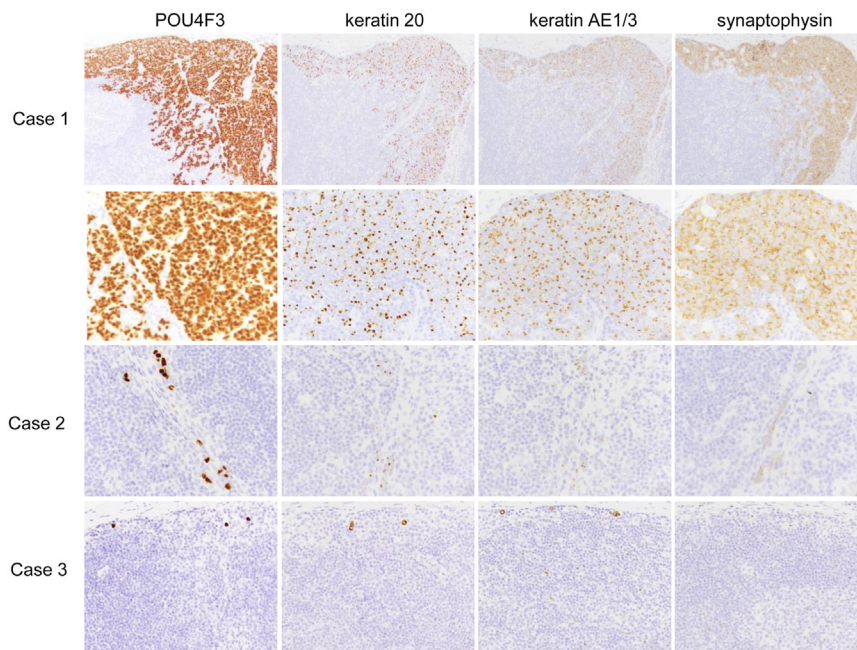


**Figure 5.**

Comparison of POU4F3, keratin 20, keratin AE1/AE3, and synaptophysin staining in sentinel lymph nodes. Case 1: Although expression of all stains is seen at low magnification, nuclear POU4F3 expression appears stronger in comparison to dot-like positivity of keratin 20 and keratin AE1/AE3. Case 2: It is easier to detect single-cell metastasis with POU4F3 in comparison to dot-like positivity of keratin 20 and keratin AE1/AE3, and weak expression of synaptophysin. Case 3: Nuclear POU4F3 expression is helpful in the setting of single-cell metastasis.

detected rare single tumor cells whereas keratin 20, keratin AE1/AE3, and synaptophysin were previously negative. This may be a false negative result of the SLN protocol due to the improved accuracy of the POU4F3 immunostain or a consequence of cutting deeper into the tissue blocks.

## Discussion

Thus far, a single sensitive and specific marker to detect MCC in diagnostic workup is not available. Leveraging the available bulk sequencing of approximately 26,600 (9264 solid tumors and 17,382 healthy tissues) as well as single-cell sequencing data of >600,000 single cells, MCC, and non-MCC tumors, and normal tissues of a variety of organs has allowed us to evaluate the specificity of POU4F3 in a comprehensive manner. These RNA analyses consistently showed *POU4F3* to be a highly specific marker of MCC, at bulk tumor level and at single-cell resolution. *POU4F3* preferentially expressed in MCC but not in other analyzed tumor types and normal tissues.

At the protein level, we confirmed this high specificity of POU4F3 for MCC. POU4F3 expression was not seen in the majority of tested non-MCC tumors. Of interest, POU4F3 immunostain labels all MCC, regardless of MCPyV status and keratin 20 expression. This is very helpful in clinical practice because it is difficult to distinguish MCPyV-negative MCC, keratin 20-negative MCC, and TTF1-positive MCC from high-grade NEC. The main differential diagnosis of MCC in the setting of widespread metastases is another small cell carcinoma, from lung and other internal sites. The distinction is of therapeutic importance. Molecular assays can be of help; however, these are costly tests. By molecular analyses, MCPyV-negative MCC often harbors high tumor mutational burden, UV signature, and *NF1* and *PIK3CA* mutations and lacks *KRAS* mutation in comparison to NEC.<sup>29</sup>

Gene expression studies have revealed a new model of SCLC subtypes defined by differential expression of key transcription regulators: achaete-scute homolog 1 (*ASCL1/ASH1/mASH1*), neuronal differentiation factor 1 (*NEUROD1*), POU class 2 homeobox 3 (*POU2F3*), and *YAP1*.<sup>30</sup> In an immunohistochemical study, 49 of 59 SCLCs (83%) expressed nuclear ASCL1 staining, whereas ASCL1 was completely negative in all 30 MCCs.<sup>31</sup> In another study of 28 MCCs, all were negative for ASCL1 (except one with focal ASCL1 expression).<sup>32</sup> Our study confirms the frequent expression of ASCL1 in SCLC and its absence in MCC.

Immunohistochemistry would be cost effective; however, there are overlapping staining patterns observed for MCC and SCLC. Our study shows that transcription factor POU4F3 is a cost effective distinguishing marker, staining almost all MCC cases in contrast to only rare small cell carcinomas. Of note, a limitation of our study is the small number of salivary gland small cell carcinomas. Including ASCL1 would increase the specificity of diagnosing MCC because MCC is invariably ASCL1-negative and SCLC would be ASCL1-positive in 54% to 73% of cases.<sup>30,31</sup> In our study, 1 POU4F3-positive SCLC was ASCL1-positive, supporting the utility of POU4F3 and ASCL1 combination.

In a recent study of 43 MCCs and 59 SCLCs by Vilasi et al,<sup>33</sup> ATOH1, TFAP2B, and CEACAM6 were reported to be helpful immunohistochemical markers in the distinction of MCC and SCLC. ATOH1 and TFAP2B exhibited nuclear staining in 100% and 93% of MCC cases, respectively, and none of the SCLC cases. On the other hand, CEACAM6 stained 83% of SCLC cases, and none of the MCC cases. One reason for the result differences could be attributed to the fact that Vilasi et al<sup>33</sup> used the microarray technique based on Affymetrix platform to obtain their marker lists, whereas our study was based on the analysis of data derived from RNA-sequencing or single-cell RNA sequencing. Excluding the differences resulting from the choice of platforms for measuring mRNA levels, we used a different statistical approach and a much wider



range of data from various types of cancers compared with Vilassi et al.<sup>33</sup> In other words, Vilassi et al.<sup>33</sup> used 23 MCCs and 9 SCLCs (a total of 32 samples) to obtain a list of markers, whereas we used a data set encompassing >9300 samples from 26 types of cancer to eliminate nonspecific markers for MCCs. However, in both Vilassi et al.<sup>33</sup> study and ours, *POU4F3* was identified to be differentially expressed in MCC versus SCLC.

Surgical excision followed by adjuvant radiation therapy is the front-line treatment for localized MCC disease.<sup>34</sup> Concurrent SLN biopsy is recommended for patients with clinically negative lymph nodes.<sup>35</sup> Detection of micrometastasis is important in both the treatment and staging/overall prognostication of patients with MCC. Treatment options for patients with positive SLN include complete or selective nodal dissection, adjuvant radiation therapy, or both.<sup>34</sup> Detection of micrometastasis in SLN requires a panel comprised of sensitive as well as specific immunostains. For detecting metastatic MCC, a panel of 3 antibodies (SATB2, keratin AE1/AE3, and synaptophysin) has been proposed; however, background staining is frequently seen with both SATB2 and keratin AE1/AE3.<sup>14</sup> In the setting of single-cell metastasis, diagnostic pitfalls can result in mistaking macrophages or antigen-presenting dendritic cells as tumor cells. Although specific, keratin 20 expression can be negative for up to a quarter of MCCs.<sup>5</sup> *POU4F3* detects metastatic MCCs similarly to keratin AE1/AE3 and keratin 20; however, the strong nuclear *POU4F3* expression allows the ease of diagnosing single-cell metastasis. Our study shows *POU4F3* to be a helpful diagnostic marker in the SLN evaluation for metastatic MCC.

*POU4F3* (POU domain, class 4, transcription factor 3 or Brn-3c) belongs to the POU-IV or Brn-3 transcription factor family and has been shown to play an important role in Merkel cell development.<sup>36</sup> *ATOH1* (*HATH1*) and *POU4F3* (Brn-3c) have been postulated to form a transcriptional hierarchy that drives the neuroendocrine differentiation in Merkel cells.<sup>37,38</sup> When DNA is tightly wrapped around histones, the chromatin is closed and inaccessible to the transcriptional “master regulator” *ATOH1*. *ATOH1* stimulates the expression of *POU4F3*, which can bind to closed and inaccessible chromatin. This in turn allows Merkel cell differentiation to proceed.<sup>38</sup> Normal Merkel cells and MCCs expressed *POU4F3* (Brn-3c), but not Ewing or neuroblastoma cell lines.<sup>38,39</sup> *POU4F3* staining of normal Merkel cells in our trichoblastoma cases is in line with these findings. Contrary to our results, Leonard et al.<sup>38</sup> reported *POU4F3* (Brn-3c) expression in only 62% (8/13) of MCC tumors. In addition, *POU4F3* expression was reported in lung adenocarcinoma.<sup>40</sup> These discrepancies could be due to differences in methodology. Leonard et al.<sup>38</sup> used an investigator-generated antibody, and Chai et al.<sup>40</sup> used an antibody from Sigma, whereas we used a commercial antibody from Santa Cruz Biotechnology.

In summary, our study built on prior works shows that *POU4F3* is a cost effective, sensitive, and specific clinical marker for MCC, in the distinction of MCC from histologic mimics as well as in the detection of single-cell metastasis in SLN biopsy.

#### Author Contributions

P.K. and M.P.H. performed study concept and design; P.K., J.M.P., Y.P.H., and M.P.H. developed the methodology; P.K., J.M.P., C.L.W., A.A., K.M.C., Y.P.H., and M.P.H. contributed to the acquisition, analysis, and interpretation of data; P.K., J.M.P., C.L.W., A.A., K.M.C., Y.P.H., and M.P.H. provided technical and material support; P.K. and M.P.H. drafted the original manuscript draft; P.K., J.M.P., C.L.W., A.A., K.M.C., Y.P.H., and M.P.H. revised and approved the final version of the manuscript.

#### Data Availability

All data generated or analyzed during this study are included in this published article and its supplementary information files.

#### Funding

There was no external funding for this work.

#### Declaration of Competing Interest

All authors have no financial or nonfinancial conflicts of interest to declare.

#### Ethics Approval and Consent to Participate

The study has been approved by Partners HealthCare Institutional Review Boards (protocol 2018P002057).

#### Supplementary Material

The online version contains supplementary material available at <https://doi.org/10.1016/j.modpat.2024.100627>.

#### References

1. Dika E, Pellegrini C, Lambertini M, et al. Merkel cell carcinoma: an updated overview of clinico-pathological aspects, molecular genetics and therapy. *Eur J Dermatol*. 2021;31:691–701.
2. Tetzlaff MT, Harms PW. Danger is only skin deep: aggressive epidermal carcinomas. An overview of the diagnosis, demographics, molecular-genetics, staging, prognostic biomarkers, and therapeutic advances in Merkel cell carcinoma. *Mod Pathol*. 2020;33(Suppl 1):42–55.
3. Moll R, Lowe A, Laufer J, Franke WW. Cytokeratin 20 in human carcinomas. A new histodiagnostic marker detected by monoclonal antibodies. *Am J Pathol*. 1992;140:427–447.
4. Chan JK, Suster S, Wenig BM, Tsang WY, Chan JB, Lau AL. Cytokeratin 20 immunoreactivity distinguishes Merkel cell (primary cutaneous neuroendocrine) carcinomas and salivary gland small cell carcinomas from small cell carcinomas of various sites. *Am J Surg Pathol*. 1997;21:226–234.
5. Hanly AJ, Elgart GW, Jorda M, Smith J, Nadji M. Analysis of thyroid transcription factor-1 and cytokeratin 20 separates Merkel cell carcinoma from small cell carcinoma of lung. *J Cutan Pathol*. 2000;27:118–120.
6. Byrd-Gloster AL, Koor A, Glass LF, et al. Differential expression of thyroid transcription factor 1 in small cell lung carcinoma and Merkel cell tumor. *Hum Pathol*. 2000;31:58–62.
7. Ordóñez NG. Value of thyroid transcription factor-1 immunostaining in distinguishing small cell lung carcinomas from other small cell carcinomas. *Am J Surg Pathol*. 2000;24:1217–1223.
8. Pasternak S, Carter MD, Ly TY, Doucette S, Walsh NM. Immunohistochemical profiles of different subsets of Merkel cell carcinoma. *Hum Pathol*. 2018;82:232–238.
9. Kervarrec T, Tallet A, Miquelstarena-Standley E, et al. Diagnostic accuracy of a panel of immunohistochemical and molecular markers to distinguish Merkel cell carcinoma from other neuroendocrine carcinomas. *Mod Pathol*. 2019;32:499–510.
10. Bellizzi AM. SATB2 in neuroendocrine neoplasms: strong expression is restricted to well-differentiated tumours of lower gastrointestinal tract origin and is most frequent in Merkel cell carcinoma among poorly differentiated carcinomas. *Histopathology*. 2020;76:251–264.
11. Cheuk W, Kwan MY, Suster S, Chan JK. Immunostaining for thyroid transcription factor 1 and cytokeratin 20 aids the distinction of small cell carcinoma from Merkel cell carcinoma, but not pulmonary or extrapulmonary small cell carcinomas. *Arch Pathol Lab Med*. 2001;125:228–231.
12. Cho WC, Vanderbeck K, Nagarajan P, et al. SOX11 is an effective discriminatory marker, when used in conjunction with CK20 and TTF1, for Merkel cell carcinoma: comparative analysis of SOX11, CK20, PAX5, and TTF1 expression in Merkel cell carcinoma and pulmonary small cell carcinoma. *Arch Pathol Lab Med*. 2023;147:758–766.
13. Xu X, Roberts SA, Pasha TL, Zhang PJ. Undesirable cytokeratin immunoreactivity of native nonepithelial cells in sentinel lymph nodes from patients with breast carcinoma. *Arch Pathol Lab Med*. 2000;124:1310–1313.
14. Szumera-Ciećkiewicz A, Massi D, Cassisa A, et al. SATB2, CKAE1/AE3, and synaptophysin as a sensitive immunohistochemical panel for the detection of

- lymph node metastases of Merkel cell carcinoma. *Virchows Arch.* 2024;484: 629–636.
15. Sundqvist B, Kilpinen S, Bohling T, Koljonen V, Sihto H. Activation of oncogenic and immune-response pathways is linked to disease-specific survival in Merkel cell carcinoma. *Cancers.* 2022;14:3591. <https://doi.org/10.3390/cancers14153591>
16. Quintanal-Villalonga A, Taniguchi H, Zhan YA, et al. Multiomic analysis of lung tumors defines pathways activated in neuroendocrine transformation. *Cancer Discov.* 2021;11:3028–3047.
17. Rahman M, Jackson LK, Johnson WE, Li DY, Bild AH, Piccolo SR. Alternative preprocessing of RNA-sequencing data in The Cancer Genome Atlas leads to improved analysis results. *Bioinformatics.* 2015;31:3666–3672.
18. GTEx Consortium. The GTEx Consortium atlas of genetic regulatory effects across human tissues. *Science.* 2020;369:1318–1330. <https://doi.org/10.1126/science.aaz1776>
19. Das BK, Kannan A, Velasco GJ, et al. Single-cell dissection of Merkel cell carcinoma heterogeneity unveils transcriptomic plasticity and therapeutic vulnerabilities. *Cell Rep Med.* 2023;4:101101. <https://doi.org/10.1016/j.xcrm.2023.101101>
20. Chan JM, Quintanal-Villalonga A, Goa VR, et al. Signatures of plasticity, metastasis, and immunosuppression in an atlas of human small cell lung cancer. *Cancer Cell.* 2021;39:1479–1496.
21. Tabula Sapiens Consortium, Jones RC, Karkanas J, et al. The Tabula Sapiens: a multiple-organ, single-cell transcriptomic atlas of humans. *Science.* 2022;376:eabl4896. <https://doi.org/10.1126/science.abl4896>
22. Liao Y, Smyth GK, Shi W. The R package Rsubread is easier, faster, cheaper and better for alignment and quantification of RNA sequencing reads. *Nucleic Acids Res.* 2019;47:e47. <https://doi.org/10.1093/nar/gkz114>
23. Frankish A, Diekhans M, Jungreis I, et al. GENCODE 2021. *Nucleic Acids Res.* 2021;49:D916–D923.
24. Robinson MD, McCarthy DJ, Smyth GK. EdgeR: a Bioconductor package for differential expression analysis of digital gene expression data. *Bioinformatics.* 2010;26:139–140.
25. Butler A, Hoffman P, Smibert P, Papalexi E, Satija R. Integrating single-cell transcriptomic data across different conditions, technologies, and species. *Nat Biotechnol.* 2018;36:411–420.
26. Eide PW, Bruun J, Lothe RA, Sveen A. CMScaller: an R package for consensus molecular subtyping of colorectal cancer pre-clinical models. *Sci Rep.* 2017;7: 16618. <https://doi.org/10.1038/s41598-017-16747-x>
27. Rohart F, Gautier B, Singh A, Cao KAL. mixOmics: an R package for 'omics feature selection and multiple data integration. *PLoS Comput Biol.* 2017;13: e1005752. <https://doi.org/10.1371/journal.pcbi.1005752>
28. Ianevski A, Giri AK, Aittokallio T. Fully-automated and ultra-fast cell-type identification using specific marker combinations from single-cell transcriptomic data. *Nat Commun.* 2022;13:1246. <https://doi.org/10.1038/s41467-022-28803-w>
29. Hartsough E, Mino-Kenudson M, Lennertz JK, Dias-Santagata D, Hoang MP. Clinical next-generation sequencing panels reveal molecular differences between Merkel cell polyomavirus-negative Merkel cell carcinomas and neuroendocrine carcinomas. *Am J Clin Pathol.* 2023;159: 395–406.
30. Rudin CM, Poirier JT, Byers LA, et al. Molecular subtypes of small cell lung cancer: a synthesis of human and mouse model data. *Nat Rev Cancer.* 2019;19:289–297.
31. Ralston J, Chiriboga L, Nonaka D. MASH1: a useful marker in differentiating pulmonary small cell carcinoma from Merkel cell carcinoma. *Mod Pathol.* 2008;21:1357–1362.
32. Chteinberg E, Sauer CM, Rennspies D, et al. Neuroendocrine key regulator gene expression in Merkel cell carcinoma. *Neoplasia.* 2018;20:1227–1235.
33. Vilasi SM, Nguyen J, Wang CJ, et al. ATOH1, TFAP2B, and CEACAM6 as immunohistochemical markers to distinguish Merkel cell carcinoma and small cell lung cancer. *Cancers.* 2024;16:788. <https://doi.org/10.3390/cancers16040788>
34. Gauci ML, Aristei C, Becker JC, et al. European Dermatology Forum (EDF), the European Association of Dermato-Oncology (EADO) and the European Organization for Research and Treatment of Cancer (EORTC). Diagnosis and treatment of Merkel cell carcinoma: European consensus-based interdisciplinary guideline – Update 2022. *Eur J Cancer.* 2022;171:203–231.
35. Bichakjian CK, Olencki T, Aasi SZ, et al. Merkel cell carcinoma, version 1.2018, NCCN Clinical Practice Guidelines in Oncology. *J Natl Compr Cancer Netw.* 2018;16:742–774.
36. Xiang M, Zhou L, Macke JP, et al. The Brn-3 family of POU-domain factors: primary structure, binding specificity, and expression in subsets of retinal ganglion cells and somatosensory neurons. *J Neurosci.* 1995;15: 4762–4785.
37. Yu HV, Tao L, Llamas J, et al. POU4F3 pioneer activity enables ATOH1 to drive diverse mechanoreceptor differentiation through a feed-forward epigenetic mechanism. *Proc Natl Acad Sci U S A.* 2021;118:e2105137118. <https://doi.org/10.1073/pnas.2105137118>
38. Leonard JH, Cook AL, Gele MV, et al. Proneural and proneuroendocrine transcription factor expression in cutaneous mechanoreceptor (Merkel) cells and Merkel cell carcinoma. *Int J Cancer.* 2002;101:103–110.
39. Jarvis JE, Miao L, Hallaert P, et al. POU4F3 is necessary for normal Merkel cell formation, whereas POU4F1 is dispensable. *J Invest Dermatol.* 2024; S0022-202X(24)01890-6. <https://doi.org/10.1016/j.jid.2024.06.1284>
40. Chai X, Ding X, Lyu X, et al. POU4F3 acts as a tumor suppressor in lung adenocarcinoma via the endoplasmic reticulum stress signaling pathway. *J Cancer.* 2022;13:554–564.